January 2014

Langerhans Cell Contributions To Ultraviolet Light-Induced Cutaneous Carcinogenesis

Marianna Freudzon
Yale School of Medicine, marina.freudzon@yale.edu

Langerhans Cell Contributions to Ultraviolet Light-Induced Cutaneous Carcinogenesis

A Thesis Submitted to the

Yale University School of Medicine

in Partial Fulfillment of the Requirements for the

Degree of Doctor of Medicine

by

Marianna Freudzon

2014

LANGERHANS CELL CONTRIBUTIONS TO ULTRAVIOLET LIGHT-INDUCED CUTANEOUS CARCINOGENESIS. Marianna Freudzon, Julia Lewis, Renata Filler, and Michael Girardi. Department of Dermatology, Yale University, School of Medicine, New Haven, CT.

Epidermal dendritic cells, called Langerhans cells (LC), were recently shown to facilitate DMBA/TPA-induced chemical carcinogenesis. LC contribution to UV-induced carcinogenesis, however, remains to be elucidated. We used the Langerin-DTA transgenic mouse model that lacks LC to characterize early and late effects of DNA damage in epidermis following exposure to UVB light. We found that LC density in LC-intact mice remains unchanged at 1hr and 24hr post 100 J/m^2 UVB, suggesting that LC are poised to affect the surrounding epidermal cells following acute low-dose UVB exposure. During this time interval, LC-deficient mice had significantly fewer γH2Ax-positive cells within the epidermis, indicative of decreased UV-induced DNA damage in the absence of LC. However, when the pathognomonic direct and indirect UV-induced DNA lesions were measured (cyclobutane pyrimidine dimers and 8-oxoguanine, respectively), we found no differences in the absence or presence of LC, suggesting that LC may contribute to acute UV-induced DNA damage by a different, unidentified mechanism. Since mutant p53, a tumor suppressor protein highly associated with squamous cell carcinoma, arises from unrepaired DNA damage, we measured islands of clonally expanded keratinocytes harboring mutant following chronic UVB exposure. LC-deficient mice had significantly fewer p53 islands and a two-fold decrease in the total area occupied by p53 islands after 9 weeks of UVB irradiation, thus LC also contribute to the survival and proliferation of transformed keratinocytes during chronic UVB exposure. Collectively, these results suggest that LC influence DNA damage and clonal expansion in the surrounding epidermal cells in both acute and chronic UVB exposure. It provides new insight into the previously unknown role of LC in photocarcinogenesis with the objective to develop novel preventive and therapeutic targets against skin cancer.

Acknowledgements

As a scientist, I am skeptical of the fortunes of luck. Nevertheless, coincidences have certainly steered me toward the accomplishments that I have had thus far. Many of the people below have come into my life by chance. Yet their belief in my potential opened doors and allowed me to seize opportunities that led me higher and farther than I could have imagined. For this, I am lucky and I thank them dearly:

- Michael Girardi, for being my mentor and true example of a physician-scientist. Thank you for your guidance in establishing a career where I can combine challenging clinical medicine with basic science research.
- Julia Lewis, for providing knowledge, balance, and support in the lab. Thank you for answering my many daily questions, however naïve, without a hint of impatience.
- Mama and Papa, for your love and support. Thank you for your weekly catering and laundry services throughout medical school.
- Leon, my brother, for plowing the path to both our success. It's all in the genes!
- Juanpa, for sharing long hours working hard and traveling harder.
- Laurinda Jaffe, for inspiring me in the fascinating and microscopic world of cell biology. Thank you for continuing to be my mentor and friend.

I would also like to thank the Yale School of Medicine and Office of Student Research for making my research year possible with funding from the Clinical and Translational Science Award provided by the National Institute of Health. I will dedicate my career to serving those who will need my help and extending the boundaries of human knowledge to give merit to what you have graciously offered to me.

Table of Contents

Table of Figures

Introduction

Langerhans cell discovery and functional roles

Langerhans cells (LC) were first described by Paul Langerhans who eloquently detailed their dendritic appearance using light microscopy in his 1868 paper "On the nerves of the human skin" (1). It was postulated that LC were sensory nerve endings based on their morphology and location in the epidermis (1, 2). After a century of scientific dispute, scientists recognized the immunological importance of LC by their presence in histiocytosis X (renamed LC histiocytosis), similarities in intracellular structures to macrophages (3), ability to move across the basement membrane into the dermis (4, 5) and draining lymph nodes (6), and the presence of immunologic surface markers such as major histocompatibility complex (MHC) (7, 8) and Fc and C3 receptors (9).

Over the past two decades, new immunological discoveries have further broadened yet complicated our understanding of these unique cells. It is now well established that LC are a self-proliferating subset of immature dendritic cells (DC) residing in the epidermis (10, 11). They reside predominantly within the suprabasal layer and can occasionally be found in other nucleated epidermal layers in humans (12). Their dendrites, however, surround the constantly differentiating keratinocytes (KC), even extending superficially and penetrating through KC tight junctions to just under the stratum corneum, to form a dynamic mesh that surveys the extent of our skin surface (13, 14). Mice and other mammals (but not humans) have an additional epidermal immune cell population with strikingly similar dendritic morphology, called dendritic epidermal T cells (DETC) that express the γδ T cell receptor on their surface (15). In mice, LC and

DETC dendrites together form a spatially extensive immune structure in order to communicate with each other and the surrounding keratinocytes within the epidermis. This cellular network is at the forefront in mounting an adaptive immune response against antigens that LC phagocytose (16) and present to T cells (17). As antigen presenting cells (APC), LC have been reported to induce a strong $CD4^+$ helper T cell response, important for cell-mediated immunity (18). Evidence supports that LC can also cross present and activate $CD8^+$ cytotoxic T cells. The importance of cross presentation for immunity against some tumors and viruses as well as establishing tolerance to self has encouraged scientists to study whether LC may be used in cancer treatment, the development of vaccines, and other forms of immunotherapy (19, 20).

Recent advances in LC biology, however, have shifted the notion that LC are solely responsible for mounting and augmenting an immunological response to antigens. The novel discoveries were made possible by the creation of several genetically modified murine models that take advantage of the Langerin gene. Langerin is a highly-specific LC transmembrane protein (21), although other Langerin-positive DC have recently been described (22). A Langerin-DTA (Lang-DTA) transgenic mouse model was created by the insertion of a bacterial artificial chromosome that used the human Langerin promoter to drive expression of the cytotoxic subunit A of diphtheria toxin (DTA) in order to effectively and constitutively deplete LC in the epidermis, while other $Langerin^+$ DC remain unaffected (23). These Lang-DTA mice show a paradoxical increase in a contact hypersensitivity response. In contrast to previous *in vitro* functional studies that pointed to a primarily immunogenic role for LC in promoting $CD4^+$ and $CD8^+$ T cell responses, these *in vivo* depletion studies suggest that LC also play a down-regulatory role,

suppressing an exacerbated immune reaction to antigens (23). There are many reasons why this functional effect may be important in the epidermis. For one, as skin is at the interface with the environment, peripheral tolerance to small amounts of benign antigens as well as self-antigens is essential in order to maintain the physical barrier and prevent autoimmunity (24).

LC implication in chemical carcinogenesis

Interestingly, in the past five years, research using this Lang-DTA mouse model has elucidated a new, apparently paradoxical role that may be the unintended effects of industrialization byproducts on these superficially located cells. Although their ability to cross present and to activate cytotoxic T cells might predict protection against tumor cells, their down-regulatory role observed in the studies above suggested that alternative functional consequences of their absence would certainly be possible. To address the unknown contribution of LC in carcinogenesis, a two-step chemical carcinogenesis assay was performed, whereby a tumor mutagen, 7,12-dimethylbenz[a]anthracene (DMBA), was applied to mouse skin, followed by repeated application of a proinflammatory tumor promoter, 12-O-tetradecanoylphorbol 13-acetate (TPA) (25, 26). DMBA is a potent tumorigenic chemical closely related in structure and function to polycyclic aromatic hydrocarbons (PAHs), including benzo[a]pyrene (BaP). PAHs are created by the incomplete combustion of fossil fuels and wood, thus ubiquitously found in industrial air pollutants, coal tar, cigarette smoke, automobile exhaust, and smoked foods (27). This well-established carcinogenesis method has been shown to cause the development of squamous cell carcinomas (SCC) in various mouse strains (28, 29). Lang-DTA mice,

however, remain profoundly resistant regardless of the absence or presence of DETC, suggesting that LC independently mediate chemical carcinogenesis (30). This begs the question of mechanism. DMBA causes bulky DNA lesions that preferentially target an adenosine to tyrosine activating point mutation in codon 61 of the *Hras* oncogene, thus initiating mutagenesis and subsequent carcinogenesis (31). Using the biomarker of DNA damage γH2Ax, a phosphorylated histone that gets recruited to areas of focal DNA lesions (32), it was also shown that Lang-DTA mice exhibit significantly less $\gamma H2Ax^{+}$ keratinocytes after exposure to DMBA (30), suggesting that LC may increase DMBA-induced carcinogenesis by augmenting its DNA damage potency.

Ultraviolet light-induced cutaneous cancers

Ultraviolet light (UV) is also a known carcinogen (33). Numerous epidemiologic and scientific studies support that UV exposure from solar radiation and tanning beds causes basal cell carcinoma (34, 35), squamous cell carcinoma (36, 37), melanoma (38, 39), and Merkel cell carcinoma (40). Scientists in the late 19^{th} and early 20^{th} centuries were the first to note that chronic sun exposure leads to the development of skin cancer by observing their high incidence in farmers and sailors (41, 42). This launched a flurry of photocarcinogenesis investigation using animal models and epidemiologic research.

Currently, nonmelanoma skin cancers (NMSC), including basal cell (BCC) and squamous cell carcinoma (SCC), are the most common malignancies in the United States. They have a substantial impact on patient morbidity and although metastases are rare, ranging from 0.0028% to 0.55% in patients with BCC, they carry a poor prognosis and high mortality (43, 44). Skin malignancies also remain among the most costly cancers to

treat following lung, prostate, colorectal, and breast (45). Furthermore, numerous studies have shown that incidence of skin cancer is increasing dramatically both in the United States (46, 47) and internationally (48, 49). It is postulated that the rising incidence of skin cancer is caused by increased occupational and recreational sun exposure, depletion of the ozone layer, extended longevity, and immunosuppression induced by pharmaceutical drugs or diseases such as AIDS. Organ transplant recipients who are on long-term immunosuppression are particularly susceptible to squamous cell carcinoma (50). This myriad of external contributors augments the risk of deregulation within basal and follicular keratinocytes, which are the cells that give rise to NMSC. Human skin, however, also consists of other cells, including LC, Merkel cells, and melanocytes, all of which are located within reach to sense and respond to UV exposure. What are the skin's intrinsic contributors to NMSC? Few have addressed this question, yet our new evidence to support LC contribution to chemical carcinogenesis gives reason to investigate their possible role in UV-induced carcinogenesis.

UV light is only a portion of the solar radiation spectrum, spanning from 400 nm to 100 nm. It is subdivided roughly based on its mutagenic and clinical significance into UVA (400 – 315 nm), UVB (315 – 280 nm), and UVC (280 – 100 nm). As a chromophore, DNA absorbs light maximally at 260 nm, making UVC the most mutagenic and lethal to cells (51). Almost all UVC light that is emitted by solar radiation, however, is absorbed by ozone and oxygen within our atmosphere and does not pose any clinical significance (52). Of the terrestrial UV light that penetrates through the atmosphere, it is estimated that 80 – 90% consists of UVA, while the remaining 10 – 20% is UVB. Although we are exposed to significantly less UVB, it is more readily absorbed

by DNA and, therefore, more contributory to mutagenesis (53). Nevertheless, UVA and UVB light occur along a continuum. UVA also causes genotoxic and mutagenic effects in keratinocytes, however, to a lesser extent than UVB (54) and plays a role in melanoma and non-melanoma skin cancer (55). Interestingly, recent studies further showed that bordering wavelengths between UVA and UVB may bring about more mutagenic load due to diminished apoptosis induction (56).

Direct and indirect UV-induced DNA damage

The stepwise cascade of events that leads to UV-induced carcinogenesis begins with DNA damage. UV light causes DNA damage by direct and indirect mechanisms (Fig. 1). UV energy can be directly absorbed by nucleotides within DNA, causing them to achieve an excitable state and their consequent conversion to photoproducts (57). Cyclobutane pyrimidine dimers (CPD), which include thymine-thymine and thymine-cytosine dimers, make up the majority (80%) of photoproducts created by the direct pathway (58). 6,4-photoproducts and their conversion to Dewar valence isomers account for the rest of the direct lesions (59). Both CPD and 6,4-photoproducts have been associated with mutagenesis and tumor formation (60, 61).

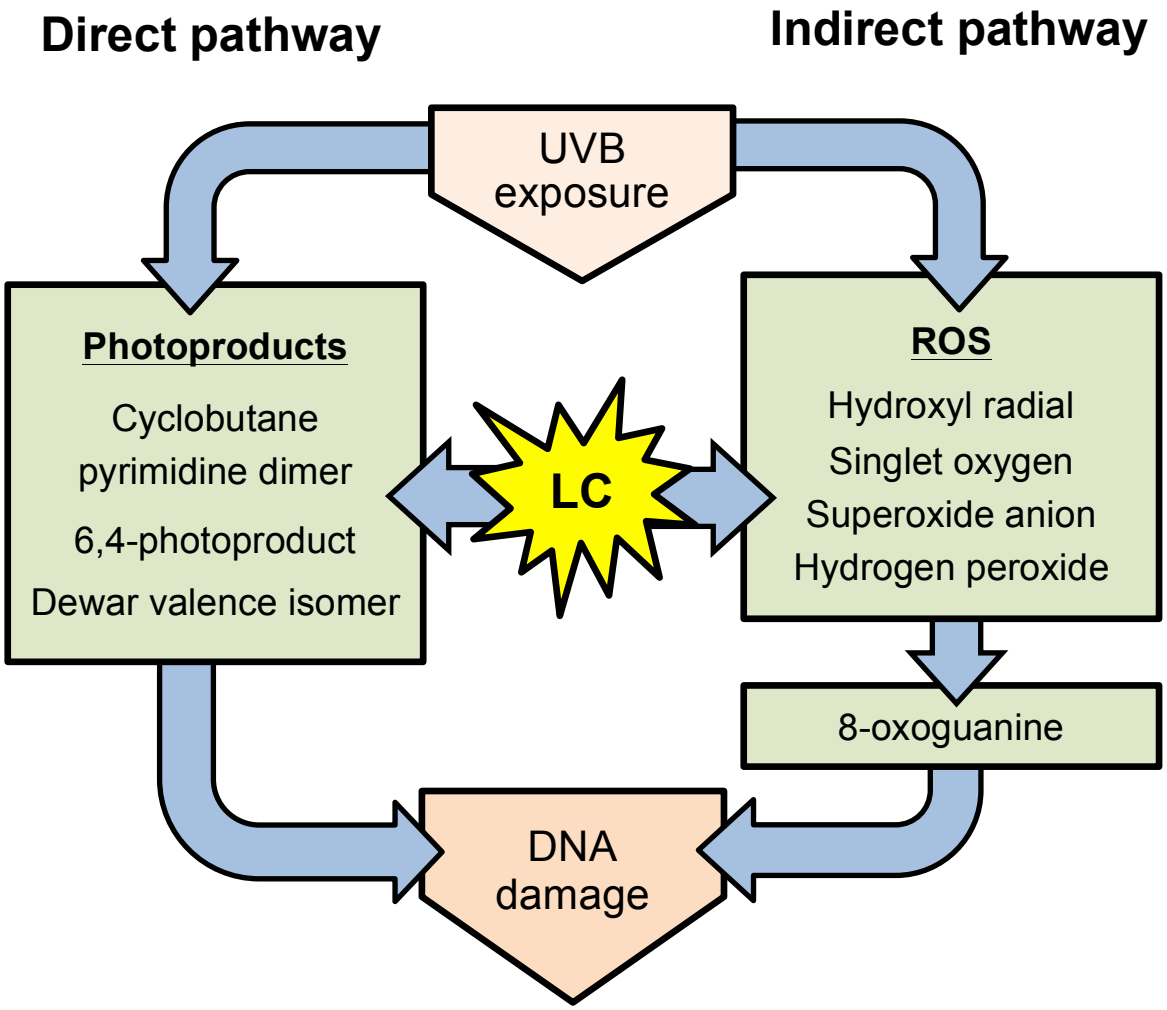

Figure 1. Exposure to UVB light causes DNA damage by two major pathways. Directly, by the creation of dimerized photoproducts, the most common of which are cyclobutane pyrimidine dimers (CPD), which amount to 80% of direct DNA lesions. And indirectly, by the production of reactive oxygen species (ROS) that oxidize DNA-incorporated and cytoplasmic nucleotides, the most common of which and of proven mutagenicity is 8-oxoguanine (8-oxoG).

The indirect pathway to DNA damage is caused by the absorption of photon energy by oxygen molecules within the cell, thereby creating reactive oxygen species (ROS) (62-64). Most commonly created ROS within UV-irradiated cells include hydroxyl radial (•OH), singlet oxygen ($^1O_2$), superoxide anion ($•O_2^-$), and hydrogen peroxide (H_2O_2) (65). These highly reactive molecules attack proteins, lipids, and DNA within cells, inducing a significant amount of structural and regulatory damage that, collectively, is termed oxidative stress. ROS cause the oxidation of cytoplasmic and DNA-incorporated nucleotides that create pathognomonic lesions, the most common of which and of proven mutagenicity is 8-oxoguanine (66, 67).

Species developed molecular mechanisms to protect against UV-induced DNA lesions, namely by various DNA repair pathways. These repair machinery, however, are not without their inaccuracies. With repeated UV irradiation (accumulated over our life spans), we accumulate DNA lesion misrepair. Mutagenesis results when misrepaired lesions may activate oncogenes or deactivate tumor suppressor genes allowing cells to gain autonomy at the expense of the surrounding tissues and whole organism function. The classic tumor suppressor gene p53 is important in the initiation of transcriptional regulation, arresting the cell cycle until DNA repair is complete, and inducing apoptosis, if DNA is irreparable (68). Mouse models with a genetic deletion of normal p53 are more susceptible to the spontaneous formation of tumors (69) and mutated p53 has been implicated in 90% of non-melanoma skin cancers (70). Signature UV-induced CC → TT and C → T mutations within the p53 gene have implicated UV irradiation as the major inducer of mutations in squamous cell carcinoma (71). Interestingly, the paradigm that p53 acts as a classic tumor suppressor gene has changed in the past ten years with the

discovery that some gain-of-function mutations promote tumorigenesis independent of wildtype p53 (72). Thus, mutant p53 may not only lose its ability to arrest cell cycle and induce apoptosis, but may also play a role in tumor promotion itself through independent oncogenic processes.

To study whether LC contribute to UV-induced tumor initiation and promotion, we used Lang-DTA transgenic mice to compare the level of DNA damage that occurs acutely following UV exposure in LC-intact versus LC-deficient skin. We further characterized the type of DNA damage that occurs by quantifying direct CPD and 8-oxoguanine formation, and measuring the production of ROS within keratinocytes co-cultured with UVB-irradiated LC. Lastly, to investigate the chronic effects of UV exposure, we compared the size and quantity of clonal cell clusters containing accumulated mutant p53 within keratinocytes, henceforth called p53 islands.

Hypothesis

Langerhans cells (LC) contribute to UV-induced tumor formation at various steps of carcinogenesis: acutely following UVB exposure with an increase in keratinocyte DNA damage, and upon chronic UVB exposure by promotion of the clonal expansion of keratinocytes containing mutated p53.

Specific aims

1) Compare the amount of DNA damage within keratinocytes in UV-irradiated Langerin-DTA transgenic (Lang-DTA) mice and their normal littermate controls (NLC) after acute exposure to UVB
    a. Quantify γH2Ax immunofluorescence in epidermal sheets from Lang-DTA and NLC mice at 1 hour post-UVB irradiation
    b. Compare CPD and 8-oxoguanine immunofluorescence in epidermal sheets from Lang-DTA and NLC mice at 1 and 24 hours post-UVB irradiation
2) Measure reactive oxygen species (ROS) production in UVB-irradiated LC and their ability to transfer ROS to and induce oxidative stress in keratinocytes *in vitro*
3) Quantify the number and density of p53 islands in chronically UVB-irradiated Lang-DTA and NLC mice

Methods

Animals

Langerhans cell deficient (Lang-DTA) mice on the FVB background were generated at Yale University School of Medicine. A bacterial artificial chromosome-based transgene containing human Langerin, modified to drive expression of diphtheria toxin subunit A from an internal ribosome entry site, was inserted in the 3' untranslated region of the Langerin gene (23). Hairless SKH1 mice on the FVB background were kindly provided by Dr. Donna Kusewitt (M.D. Anderson Cancer Center). These mice contain two null copies of the *hairless* (*hr*) gene, which is responsible for suppressing keratinocyte differentiation and promoting follicular development, rendering these mice completely alopecic (73). Hairless SKH1 mice were sequentially bred with hairy Lang-DTA mice and selected for the presence of the null *Hr* gene and the Lang-DTA transgene, in order to create hairless Lang-DTA mice on the FVB background. All future breeding were SKH1 with SKH1-Lang-DTA, whereby 50% of the offspring are hairless LC deficient mice (FVB-SKH1-Lang-DTA) and 50% are hairless LC intact normal littermate controls (FVB-SKH1). Genotyping was performed by PCR using DNA prepared from tail snips taken before 7 days of age, per animal care protocol. All procedures have been approved by Yale's Institutional Animal Care and Use Committee.

Photocarcinogenesis

To induce ultraviolet (UV) DNA damage, hairless DTA and NLC mice were irradiated with four UVB lamps (FS20T12-UVB, National Biological Corp., Twinsburg, OH) within a black UV-protective chamber. Lamp tube-to-target distance was

approximately 15 cm. The lamps emit an energy spectrum spanning 250 – 420 nm, consisting of 72.6% UVB, 27.4% UVA, 0.01% UVC, with peak emission at 313 nm. All UVC light was removed by irradiating mice under a UVC filter (Kodacel TA422, Eastman Kodak, Rochester, NY). A calibrated UVB fluence meter (G&R Labs Intensity Meter Model 200, UVB probe P1529) was used to determine the amount of exposure time needed for a specific dose of UVB irradiation. To correlate the amount of UVB exposure to sunlight and ensure that physiologic doses were used, 100 J/m^2 or 1 standard erythema dose (SED), was shown to be approximately fifteen minutes in direct sunlight at noontime during the summer in New Haven, CT. For clinical relevance to human solar radiation exposure, the minimal erythema dose (MED) for Fitzpatrick skin types I (pale white) to IV (moderate brown) would be expected to range from 150 – 600 J/m^2, or 1.5 – 6 SED (74).

For acute UVB exposure, mice were sacrificed at 1 and 24 hours following irradiation. For chronic UVB exposure, unrestrained mice were irradiated under a wire mesh that allowed them to move horizontally, but prevented them from standing up. To minimize erythema and scalding, UVB doses were initiated at 160 J/m^2 during the first week and were increased by 50% during subsequent weeks until a maximum dose of 400 J/m^2 was reached for the remaining time. Mice were irradiated thrice weekly (Monday, Wednesday, Friday) for a total of five or nine weeks.

Epidermal sheet isolation

To analyze samples of skin for UV-induced DNA damage and p53 island formation, epidermal sheets were isolated from Lang-DTA and NLC mice. Back body

wall (3 cm x 2 cm) was excised and subcutaneous fat was removed from the dermis by gently scrapping using closed surgical scissors. The skin was floated dermal side down over 0.5 M ammonium thiocyanate (NH_4SCN) and incubated for 20 minutes at 37°C or alternatively, for 2 hours in 20 mM ethylenediaminetetraacetic acid (EDTA) in PBS at 37°C. The epidermal layer could then be gently scraped off using forceps. The epidermal sheets were straightened and rinsed in cold PBS, fixed as intact structures in acetone at −20°C for at least 20 min and no longer than 24 hours (we found little variation within this duration range), and rehydrated in cold PBS for 30 min on ice prior to immunofluorescent staining and fluorescence microscopy.

DNA denaturation

To expose the DNA lesions for antibody binding, the DNA had to be denatured. Epidermal sheets were cut into 1 cm x 1 cm samples. For anti-CPD antibody staining, flat epidermal sheets were incubated in 0.4 M NaOH in 70% ethanol for 22 minutes at room temperature, then gently washed four times over 30 minutes with cold PBS containing 0.5% Triton X-100. We found 22 minutes to be the ideal time for denaturing DNA to achieve good CPD immunofluorescence signal without excessive tissue degradation. For anti-8oxoG staining, flattened epidermal sheets were first trypsinized in 1% trypsin for 2 minutes at room temperature, then immediately denatured in 2 N HCl for 20 minutes at room temperature. Sheets were then gently washed four times over 30 minutes with cold PBS containing 0.5% Triton X-100.

Immunofluorescence

Epidermal sheets were initially blocked in PBS, 0.5% Triton X-100, 2% BSA, and 0.6 mg/ml goat serum for 1 hour at room temperature. To further reduce nonspecific staining in 8-oxoG immunofluorescence, 5 μg/ml anti-Fc receptor antibody (anti-CD16/CD32, 0.5 mg/ml, clone 2.4G2, BD Pharmingen, San Jose, CA) was also added to the blocking solution. Sheets were stained overnight at 4°C using anti-γH2AX (1 μg/ml, clone JBW30, Millipore, Billerica, MA) for double-stranded DNA breaks; anti-thymine dimer antibody (2 μg/ml, clone H3, Abcam, Cambridge, MA) for direct DNA damage, which reacts with homothymine and thymine-cytosine heterodimers; anti-8 hydroxyguanosine antibody (5 μg/ml, close N45.1, Abcam, Cambridge, MA) for indirect DNA damage; and anti-Langerin (anti-CD207, 1.6 μg/ml, clone eBioRMUL.2, eBioscience, San Diego, CA) for LC. All antibodies were diluted in blocking solution. The remaining steps were carried out at room temperature. Sheets were washed in PBS containing 0.5% Triton X-100 for 2 hours, secondarily stained for 1 hour with Alexa568-goat-anti mouse IgG (Invitrogen, Carlsbad, CA) and DyLight488-donkey-anti rat IgG (Jackson Immunoresearch, West Grove, PA), and washed again for 2 hours. For nuclear staining, sheets were incubated with 30 – 50 nM ToPro3 (Invitrogen, Carlsbad, CA), washed for 30 minutes, mounted on slides in ProLong Gold Antifade (Invitrogen, Carlsbad, CA) and stored at -20°C prior to confocal microscopy.

Confocal microscopy and image processing

All *in situ* immunofluorescence was examined using a Zeiss LSM510 Meta confocal microscope. Ten fields were imaged at 2 mm intervals across the entire sheet (2

sheets per mouse). Each image consisted of a Z-stack that spanned 12 – 20 μm at 4 μm intervals in order to capture the entire epidermal thickness. All images were processed using ImageJ (NIH) and Volocity (Perkin Elmer) software. Masked images were created based on the nuclear staining to eliminate background and cytoplasmic fluorescence. For CPD immunofluorescence, nuclear fluorescence intensity was measured using Particle Analyzer software. For 8-oxoguanine immunofluorescence, nuclear speckles were counted using Maxima Finder software, which identifies local maxima within a set noise tolerance.

Cell culture

To analyze the oxidative stress effect of irradiated LC on keratinocytes *in vitro*, mouse LC and keratinocyte cell lines were used. RPMI 1640, DMEM, and media supplements were from Invitrogen, Carlsbad, CA unless otherwise noted. Complete RPMI (CRPMI) media was used for PAM212 keratinocyte cell line and made by supplementing RPMI 1640 with 10% heat inactivated FBS, 10mM Hepes, 1% non-essential amino-acids, 2 mM L-glutamine, 1 mM sodium pyruvate, 0.05 mM β-mercaptoethanol, and antibiotics. "XS106 media" was used for XS106 LC cell line and made by supplementing CRPMI with 5% NS46/NS47 supernatant and 0.5 ng/ml mouse GM-CSF (PeproTech, Rocky Hill, NJ). XS106 (immortalized LC) and PAM212 (immortalized keratinocyte) cell lines were kindly provided by Akira Takashima (University of Toledo). To study the cellular response under more physiological cellular conditions, primary mouse keratinocytes were also used. Primary keratinocytes were isolated by floating skin from 1 to 2 day old mouse pups on trypsin at 4°C overnight,

after which the epidermis was lifted off and disaggregated in CnT-57 media (CELLnTEC, Bern, Switzerland) supplemented with antibiotics and 5000 U/ml DNAse for 2 minutes at room temperature by manual shaking. Disassociated cells were cultured in CnT-57 media that specifically selects for basal keratinocyte survival and prevents keratinocyte differentiation.

In vitro oxidative stress measurement

To analyze LC ability to create ROS and induce oxidative stress in keratinocytes, we used CellROX Green Reagent (Molecular Probes, Eugene, OR), a membrane-permeable fluorogenic probe similar to another thoroughly described fluorescent marker of ROS, dichlorofluorescin diacetate (DCFDA), which allows for intracellular live cell measurement of oxidative stress. Upon oxidation by ROS, CellROX Green exhibits excitation/emission properties similar to Green Fluorescent Protein (485nm/520nm). XS106 cells were irradiated with UVB light as described above in photocarcinogenesis, and transferred to CellROX Green-loaded PAM212 or primary keratinocytes. Confocal microscopy was used to measure an increase in CellROX Green fluorescence within PAM212 or primary keratinocytes over time after co-culture with LC. All cells were seeded at 300,000 cells per 35mm dish and cultured at 37°C and 5% CO_2, overnight. All images were captured using a Zeiss LSM710 confocal/multiphoton microscope.

Statistical analysis

Statistical significance between experimental groups was determined using one- and two-tailed Student's t-test for unpaired data, with significance at $p < 0.05$. Graphical

data are shown with scatter plots with means or bar graphs with standard errors of the means.

Division of labor

Julia Lewis and Renata Filler performed all animal breeding with selected participation of genotyping by Marianna Freudzon. γH2Ax and p53 experiments entailing tissue preparation, immunofluorescence, microscopy, and data analysis were done by Julia Lewis. Marianna Freudzon performed parallel experiments for CPD and 8-oxoguanine entailing tissue preparation, establishment of the DNA denaturation protocol, immunofluorescence, microscopy, image processing, and data analysis. Marianna Freudzon also conducted all cell culture and *in vitro* oxidative stress measurements and analyses.

Results

LC density remains unchanged at 1 and 24 hours after 50 and 100 J/m^2 UVB exposure

It has been known for more than three decades that high doses of UV irradiation lead to transient LC depletion (75). Thus, we wanted to determine whether LC density changes acutely following UVB irradiation at lower doses that are physiologically similar to solar UV exposure. CD207-labeled LC were quantified within epidermal sheets from NLC mice that were irradiated with 0 (sham), 50, and 100 J/m^2 UVB. Although LC roundness and dendricity showed some variability throughout all samples, there was no clear distinction of LC morphology within UVB irradiated versus unirradiated skin (Fig. 2A). LC density also remained unchanged at all UVB doses tested at 1 hour after exposure (0 J/m^2: 972.3 ± 109.3, 50 J/m^2: 907 ± 143.7, 100 J/m^2: 803 ± 104.7 mean LC count/mm^2 ± SEM). Likewise, LC density at 24 hours following 100 J/m^2 UVB exposure was not significantly different (1036 ± 113.9 mean LC count/mm^2 ± SEM) (Fig. 2B). Therefore, LC remain situated to affect surrounding keratinocytes, and possibly DETC, at least within the first 24 hours after irradiation with low-dose UVB.

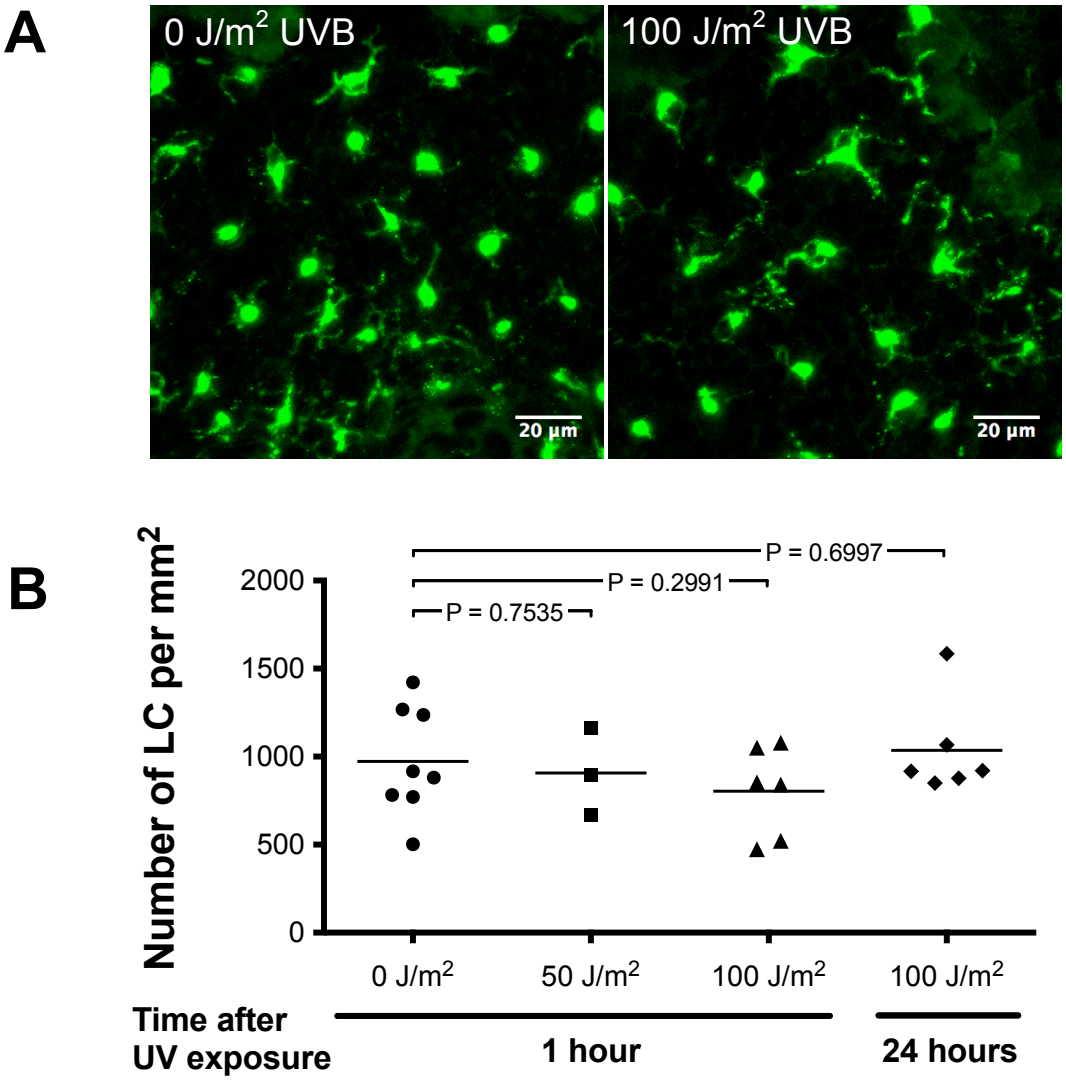

LC density (mean count per mm^2 ± SEM)			
1 hour post UVB			24 hours post UVB
0 J/m^2	50 J/m^2	100 J/m^2	100 J/m^2
972.3 ± 109.3 N=8	907.3 ± 142.7 N=3	803.3 ± 104.7 N=6	1036 ± 113.9 N=6

Figure 2. LC density does not change at 1 and 24 hours following low-dose UVB exposure. (**A**) Two examples of epidermal sheets images using confocal microscopy from NLC mice unirradiated and irradiated with 100 J/m^2 labeled with anti-CD207/Langerin (green) showing typical LC morphology and density. (**B**) LC quantification from NLC mice following 0, 50, 100 J/m^2 UVB at 1 and 24 hours post-exposure. P values (Student's *t* test) indicated in graph. Values shown in table.

LC-intact mice show significantly greater number of γH2AX$^+$ keratinocytes at 1 hr after 100 J/m^2 UVB exposure

Considering that LC are present at 1 hour after 100 J/m^2 UVB, we determined the number of keratinocytes containing γH2AX within epidermal sheets from mice irradiated with the same parameters. Interestingly, γH2AX positive keratinocytes were concentrated greatest at the suprabasal epidermal layer in close proximity to LC (Fig. 3A). Compared to NLC mice, Lang-DTA mice had significantly fewer keratinocytes containing γH2AX (130.6 ± 15.4 versus 75.7 ± 7.1 positive cell count/mm^2, P=0.0009) at 1 hour following 100 J/m^2 UVB exposure (Fig. 3B). This suggests that LC play a substantial role in the accumulation of UV-induced DNA damage in the surrounding keratinocytes, and possibly DETC, acutely after UVB exposure. Although γH2AX typically represents double-stranded DNA breaks, particularly upon exposure to ionizing radiation, it may also be recruited to other forms of DNA damage. We, therefore, decided to further characterize the type of DNA damage that occurs following acute UVB exposure in LC intact and deficient skin.

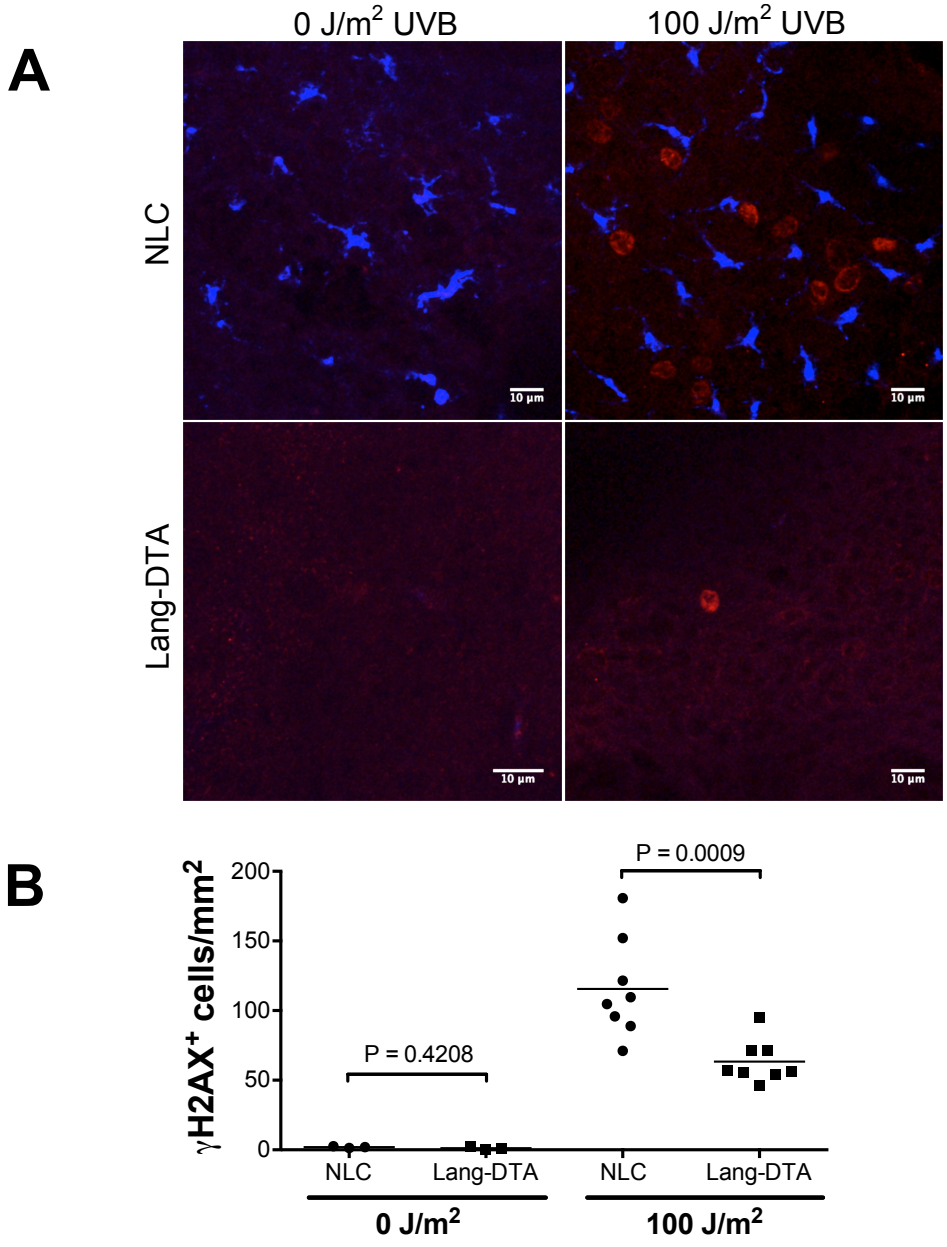

γH2AX⁺ KC density (mean per mm² ± SEM)			
0 J/m²		100 J/m²	
NLC	Lang-DTA	NLC	Lang-DTA
1.975 ± 0.3801 N=3	1.207 ± 0.782 N=3	115.6 ± 12.57 N=8	63.33 ± 5.395 N=8

Figure 3. γH2AX immunofluorescence in NLC and DTA mice following UVB exposure. NLC mice show a greater quantity of γH2AX positive keratinocytes at 1 hour after 100 J/m^2 UVB exposure at the level of LC within the epidermis. (**A**) An example of γH2AX immunofluorescence staining from an NLC epidermal sheet showing γH2AX positive nuclei (red) within several keratinocytes scattered amongst LC (blue). (**B**) Quantification of keratinocytes containing γH2AX shows a significantly less DNA damage in Lang-DTA mice. Values shown in table.

LC-intact and LC-deficient mice show a similar dose-dependent increase in CPD formation at 1 hour and 24 hours following 40, 50, or 100 J/m^2 UVB exposure

It is conceivable that LC may increase keratinocyte susceptibility to direct DNA damage or affect direct DNA repair rate. That is, LC may induce direct DNA photoproducts. To further characterize whether the UV-induced DNA damage difference between NLC and Lang-DTA mice is caused by direct or indirect mechanisms, we used *in situ* immunofluorescence to quantify CPD fluorescence intensity in Lang-DTA and NLC mouse skin at 1 and 24 hours following UVB exposure at low doses (`0 – 100 J/m^2). The data shows a sensitive and dose-dependent increase in CPD fluorescence within keratinocyte nuclei upon UVB irradiation (Fig. 4A). Using the ToPro3 nuclear counter stain and ImageJ processing, wee developed a method to accurately identify and quantify CPD fluorescence intensity within keratinocyte nuclei (Fig. 4B). We saw no significant difference, however, between NLC and Lang-DTA in CPD fluorescence intensity at 1 hour (0 J/m^2: 8.57 ± 1.76 versus 6.74 ± 2.00, 40 J/m^2: 11.29 ± 1.91 versus 13.25 ± 1.20, 50 J/m^2: 32.80 ± 1.23 versus 26.47 ± 2.74; 100 J/m^2: 60.19 ± 5.68 versus 62.72 ± 8.45 mean nuclear fluorescence in arbitrary units (AU)) and 24 hours (0 J/m^2: 14.86 ± 1.64 versus 8.68 ± 2.07, 100 J/m^2: 47.41 ± 12.21 versus 39.02 ± 2.18 mean nuclear fluorescence in AU) post-UVB exposure at all UVB doses tested (Fig. 4C), including the lowest possible dose that has been shown to induce γδ T cell activation (Adrian Hayday, personal communication). This suggests that LC do not contribute to UV-induced DNA damage by the direct pathway, which led us to test whether LC may contribute indirectly, e.g., by the creation and/or transfer of ROS to KC or the pre-conditioning the epidermal environment to oxidative stress.

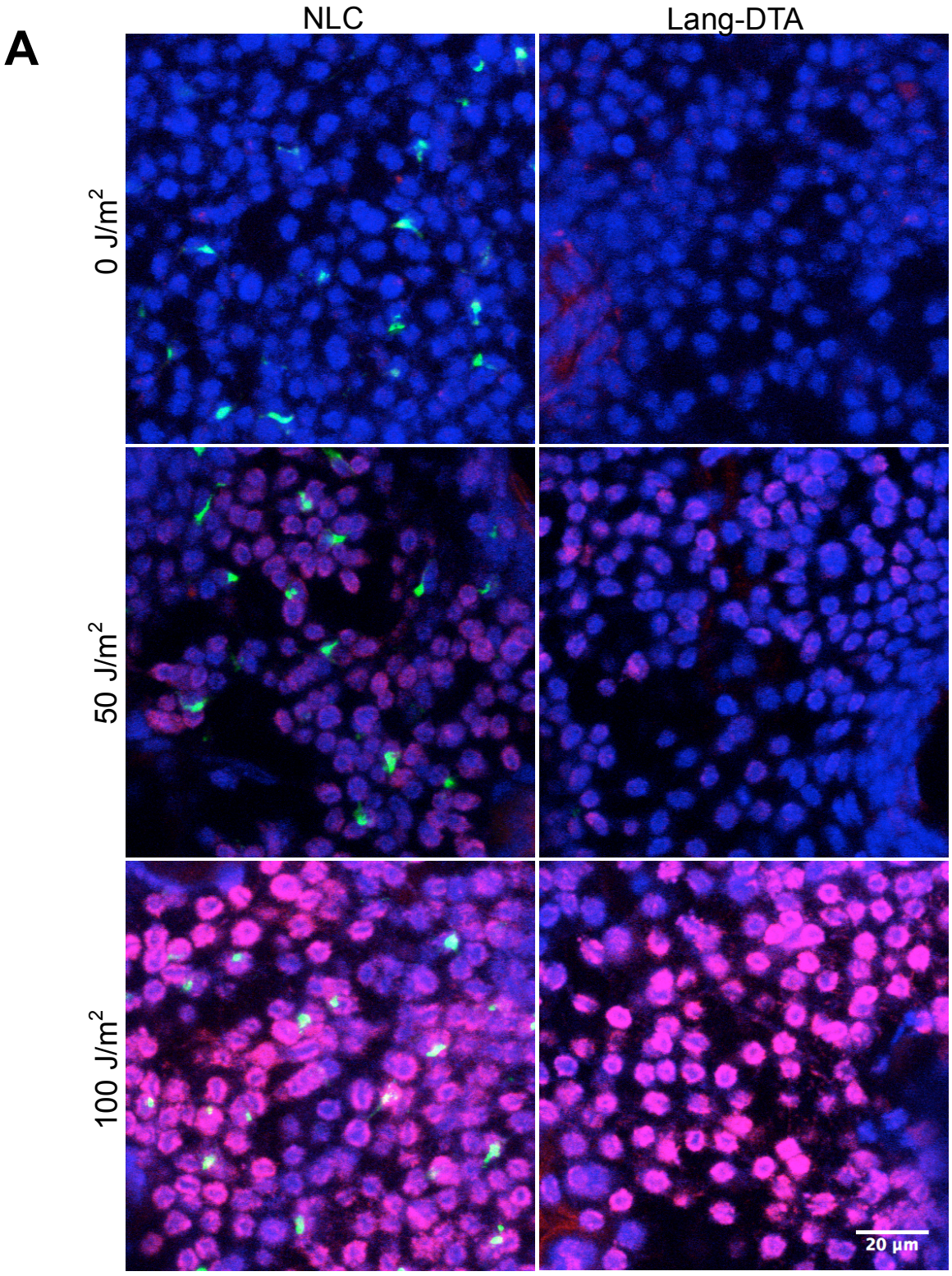

Figure 4A. Epidermal sheets from NLC and Lang-DTA mice stained with CPD for direct DNA damage (red), CD207 for Langerhans cells (green), and ToPro3 for nuclei (blue) following exposure to sham (0 J/m^2), 50, and 100 J/m^2 UVB. These images show diffuse and uniform CPD staining predominantly within keratinocyte nuclei.

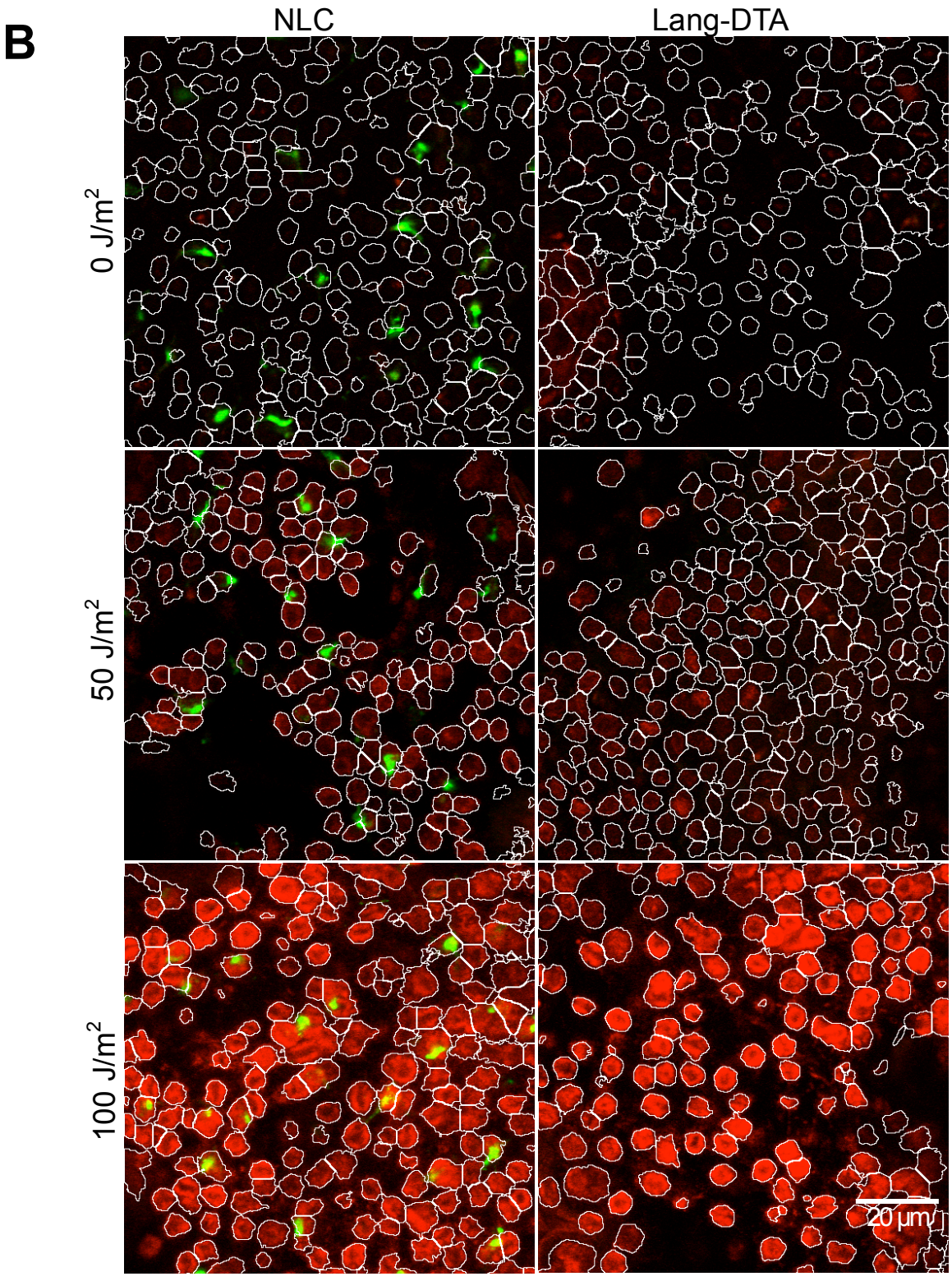

Figure 4B. Image masking for the accurate identification and quantification of CPD (red) fluorescence intensity specifically within keratinocyte nuclei. Mask was based on the ToPro3 nuclear staining, which not shown in these panels, however, is present in blue in Figure 4A).

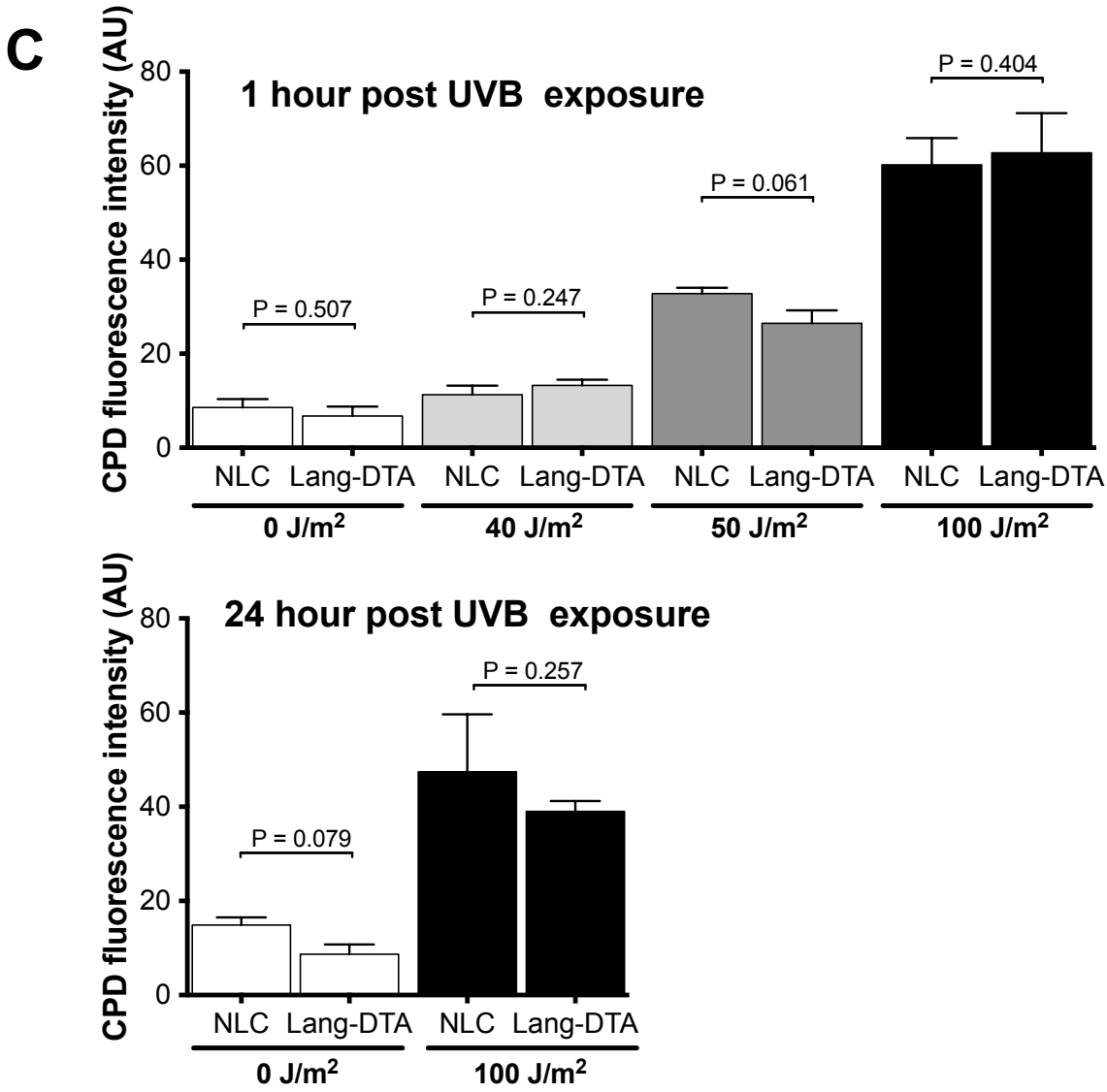

CPD fluorescence intensity (mean AU ± SEM (N))											
1hr post UVB								24hr post UVB			
0 J/m^2		40 J/m^2		50 J/m^2		100 J/m^2		0 J/m^2		100 J/m^2	
NLC	DTA	NLC	DTA	NLC	DTA	NLC	DTA	NLC	DTA	NLC	DTA
8.57 ± 1.76 (8)	6.74 ± 2.00 (6)	11.29 ± 1.91 (5)	13.25 ± 1.20 (3)	32.80 ± 1.23 (3)	26.47 ± 2.74 (4)	60.19 ± 5.68 (6)	62.72 ± 8.45 (6)	14.86 ± 1.64 (3)	8.68 ± 2.07 (3)	47.41 ± 12.21 (6)	39.02 ± 2.18 (6)

Figure 4C. CPD fluorescence intensity data comparing NLC and DTA mouse epidermis following exposure to sham (0 J/m^2), 50, and 100 J/m^2 UVB at 1 and 24 hours post-UVB exposure. CPD fluorescence intensity was quantified within nuclei and suggests a sensitive and dose-dependent increase at 1 hour post-exposure. At 24 hours following UVB irradiation, CPD fluorescence intensity begins to decrease. No significant difference in CPD fluorescence intensity was noted at any dose and time following UVB exposure. Values shown in table.

Oxidative stress may increase within KC co-cultured with UVB irradiated LC

In order to test whether UVB irradiated LC may induce oxidative stress within surrounding keratinocytes, we measured the increase in fluorescence of CellROX Green-loaded KC that were co-cultured with 0 or 800 J/m^2 irradiated LC over time (Fig. 5A). We observed a rapid increase in fluorescence intensity in KC while in the presence of 800 J/m^2 irradiated LC as compared to unirradiated LC (Fig. 5B). Co-culturing KC in irradiated media alone, however, also significantly (although inconsistently) increased fluorescence intensity within KC, suggesting the UVB exposed media itself may transfer ROS products to cells. Furthermore, over the course of our experiments we discovered that irradiating CellROX Green itself induces an increase in fluorescence and that since CellROX Green is membrane permeable, it may be washed out of cells, thereby resulting in an artificial decrease in fluorescence intensity. More work must, therefore, be done to optimize the current method. Nevertheless, because of the variability we observed in our results and the difficulty to accurately capture transient ROS activity, we decided to investigate the indirect UV-induced DNA damage pathway at a later step by assessing a product of cellular oxidative stress and the most common oxidative DNA lesion, 8-oxoguanine.

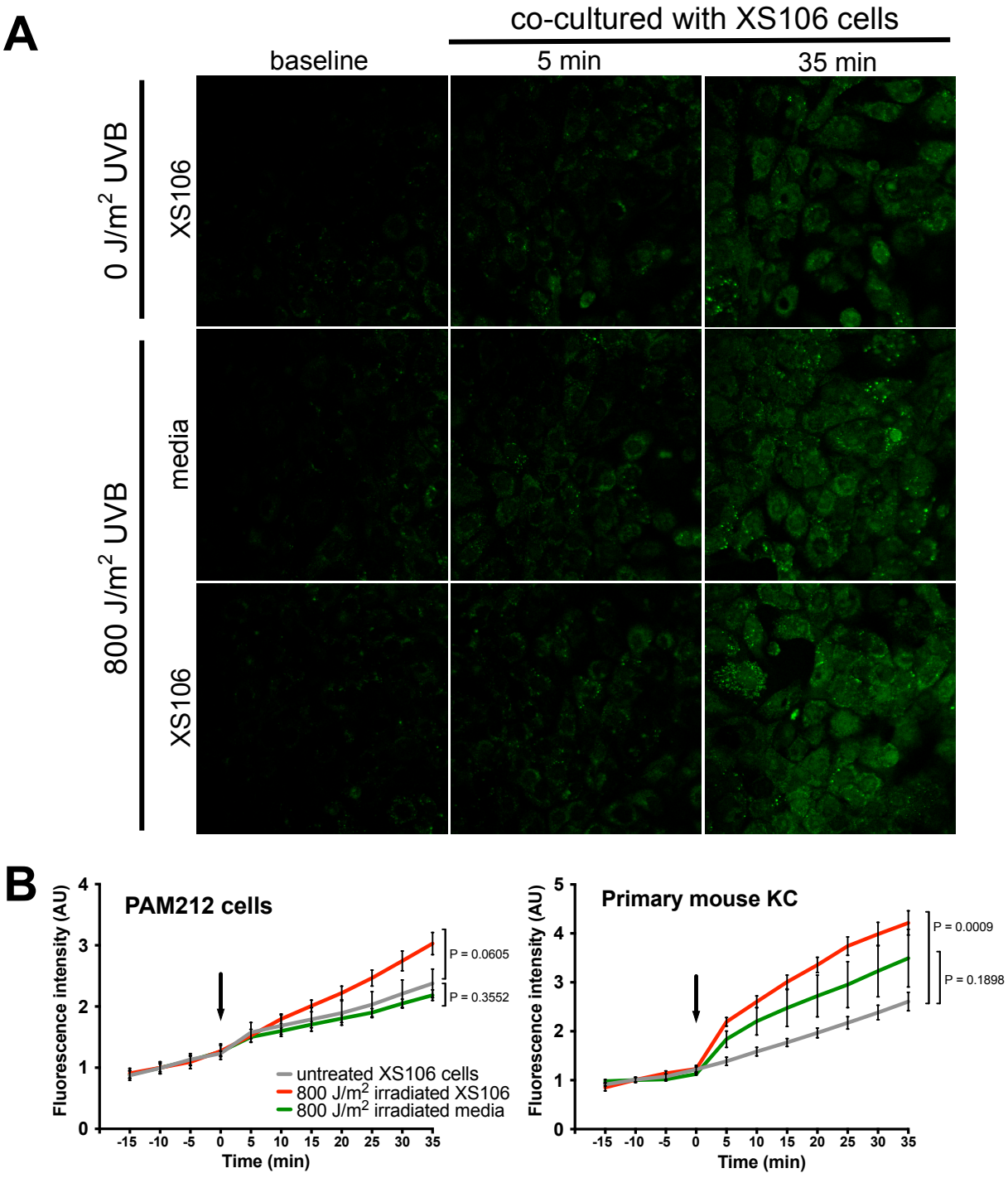

Figure 5. (**A**) CellROX Green loaded into PAM212 cells was used as an indicator for intracellular oxidative stress following co-culture with 0 or 800 J/m^2 UVB irradiated XS106 cells or with 800 J/m^2 UVB irradiated media alone. Fluorescence intensity increased over time after initiation of co-culture. (**B**) CellROX Green fluorescence intensity within PAM212 and primary mouse KC co-cultured with irradiated XS106 cells (red line), irradiated media (green line), or unirradiated XS106 cells (gray line). Black arrow indicates transfer of XS106 cells to PAM212 or primary mouse KC and beginning of co-culture. P values are comparing fluorescence intensity at final time point only (T=35 min).

LC-intact and LC-deficient mice show no detectable difference in 8-oxoguanine formation at 1 hr, regardless of UVB exposure

LC may also induce their effect on keratinocyte UV-induced DNA damage indirectly through oxidative DNA damage. We investigated this by quantifying 8-oxoguanine fluorescence intensity in Lang-DTA and NLC mouse skin at 1 and 24 hours after 800 J/m^2 UVB light. The immunofluorescence staining pattern of 8-oxoguanine showed a nuclear speckling pattern (Fig. 6A). It is consistent with other studies demonstrating the nuclear colocalization of OGG1, the major DNA glycosylase involved in initiating base excision repair of oxidized nucleotides such as 8-oxoguanine repair, and SC35, a specific marker of nuclear suborganelles, following UVB exposure (1, 76). Our data, however, suggested no significant difference in 8-oxoguanine nuclear lesions between NLC and Lang-DTA mice (0 J/m^2: 36217 ± 5163 versus 31824 ± 8684, 800 J/m^2: 32580 ± 3263 versus 31003 ± 3225 mean lesion count/mm^2) (Fig. 6B). This may suggest that LC do not contribute to UV-induced DNA damage. Because of the substantial amount of 8-oxoguanine lesions present within the unexposed skin, we must consider that the chemical method by which the epidermis is separated from the dermis prior to fixation may itself be introducing a significant amount of oxidative stress. Therefore, the epidermal sheet procedure may be saturating the skin with 8-oxoguanine lesions so that a difference is not detectable and other forms of epidermal sheet processing need to be developed to confirm this.

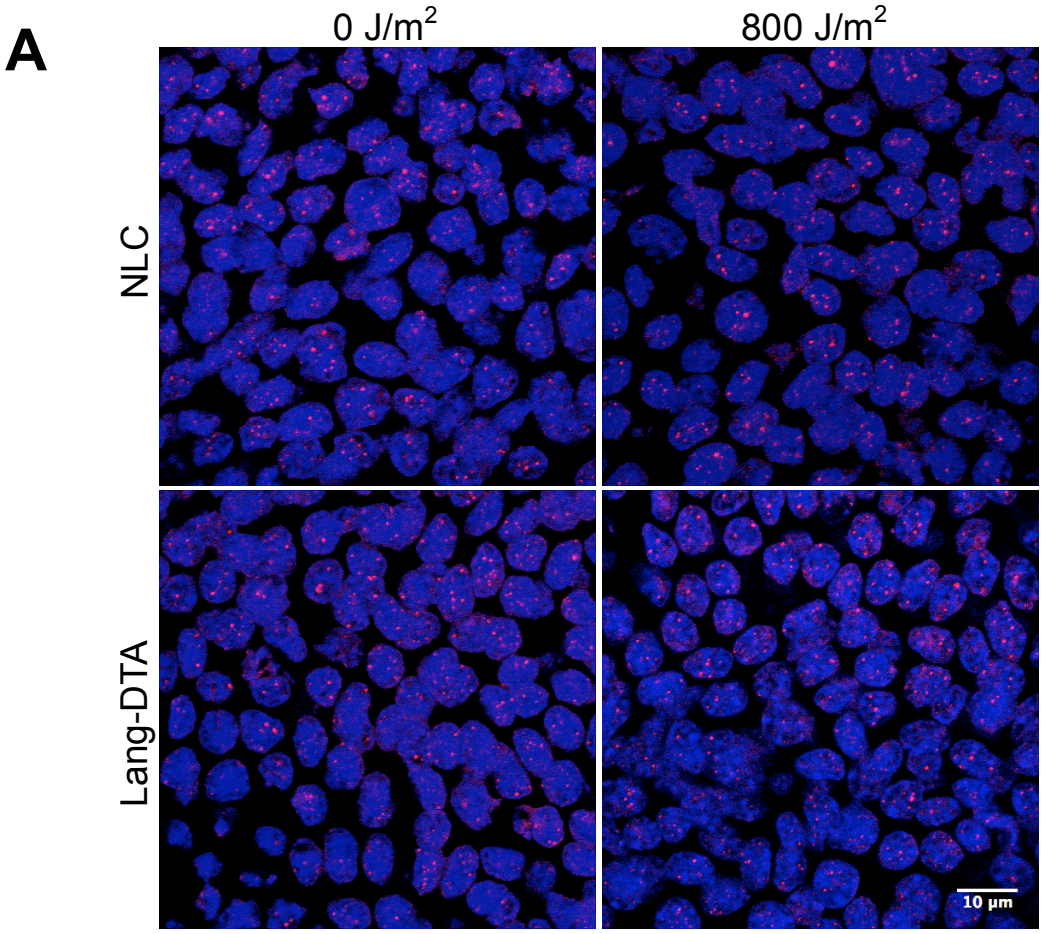

8-oxoguanine lesions (mean per mm^2 ± SEM, N)			
0 J/m^2		800 J/m^2	
NLC	Lang-DTA	NLC	Lang-DTA
36317 ± 5163 N=4	31824 ± 8684 N=4	32580 ± 3263 N=8	31003 ± 3225 N=7

Figure 6. NLC and DTA mouse epidermal sheets following sham (0) and 800 J/m^2 UVB exposure that were stained with 8-oxoguanine for indirect DNA damage (red) and ToPro3 for nuclei (blue), LC were not labeled. (A) 8-oxoG lesions appear speckled within keratinocyte nuclei. (**B**) Mean number of 8-oxoG lesions remains statistically unchanged in both NLC and DTA mice regardless of UVB exposure. Values are shown in table below.

LC-intact mice have significantly greater number and area occupied by keratinocytes containing mutant p53 following 9 weeks of chronic UVB exposure

To determine LC contribution to the chronic effects of UV-induced carcinogenesis, we measured the number and size of p53 islands in NLC and Lang-DTA skin. Although some studies have shown that extremely high doses of UVB irradiation induce LC depletion most severely at 2 days after exposure, at approximately 2 weeks, the epidermis is repopulated by hematopoietic monocyte precursors that reestablish the LC network and thus may continue to exert effects on the surrounding keratinocytes (1, 2, 77). Following 9 weeks of chronic UVB exposure, NLC mice showed a two-fold increase in the total p53 island area (8556 ± 1454 versus 4255 ± 539 μm^2; $P<0.0098$), and a significantly greater number of p53 islands (78.95 ± 11.50 versus 51.19 ± 3.17; $P=0.0003$) per mm^2 of skin, as compared to Lang-DTA mice (Fig. 7, A and B).

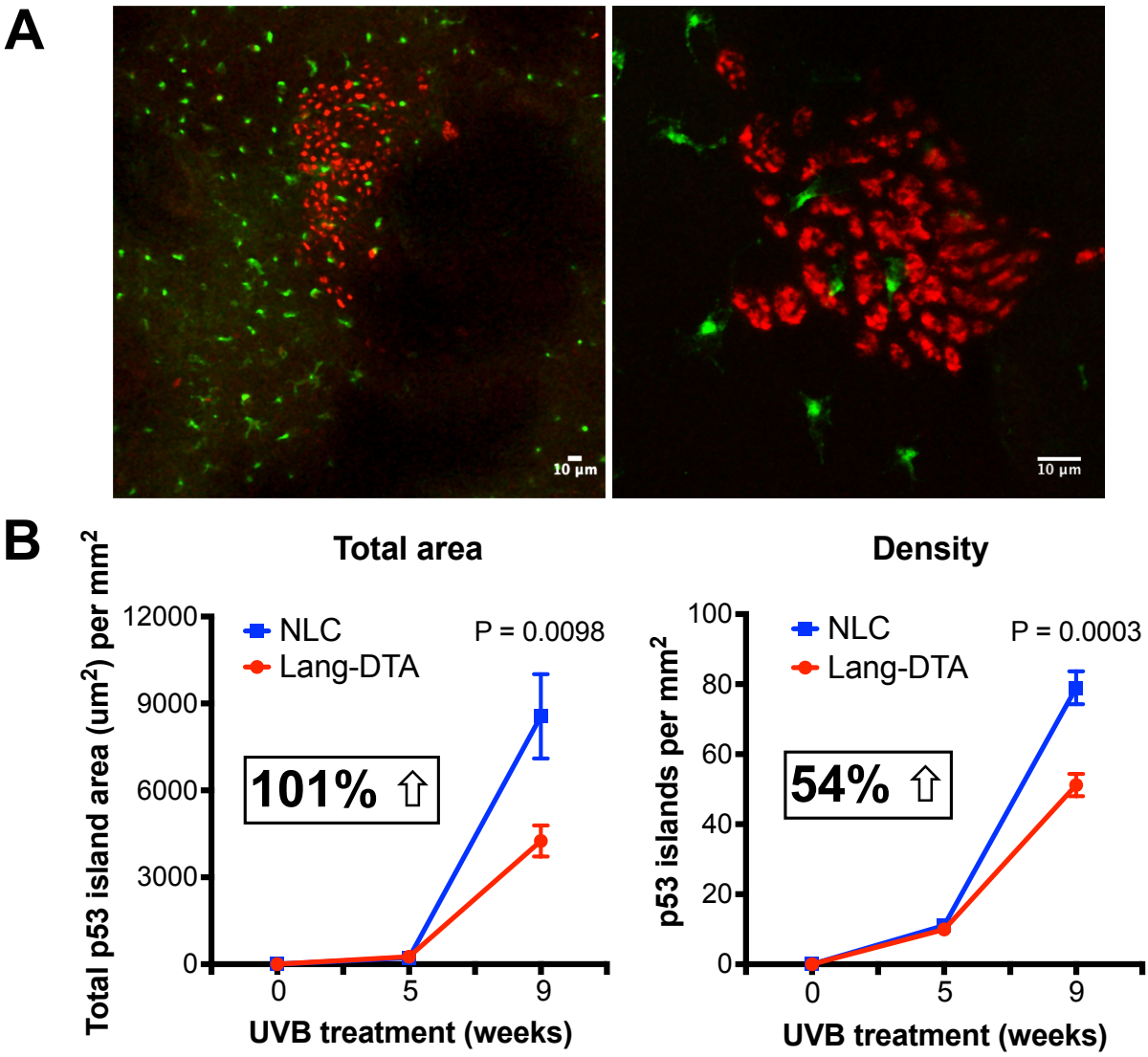

p53 island area (µm/mm² ± SEM)		p53 islands (mean per mm² ± SEM)	
NLC	Lang-DTA	NLC	Lang-DTA
8556 ± 1454 N=6	4255 ± 539 N=6	78.95 ± 11.50 N=6	51.19 ± 3.17 N=6

Figure 7. p53 island number and density following chronic UVB exposure. NLC and DTA were exposed to UVB light for 5 or 9 weeks, after which the epidermal sheets were stained for p53 protein. Clonal cells with dysfunctional p53 will overexpress and accumulate p53 protein while continuing to replicate due to the inability to arrest mitosis or induce apoptosis, forming p53 islands (red). LC (green) were also found to infiltrate into the p53 islands. (**A**) Examples of p53 islands from NLC mouse epidermal sheets at two different magnifications demonstrating close association of keratinocytes containing mutant p53 and infiltrating LC (**B**) Chronically irradiated NLC mice were found to have significant greater number and size of p53 islands at 9 weeks, but not at 5 weeks.

Discussion

Langerhans cells have traditionally been considered the antigen presenting cells of the skin, primarily important in mounting an adaptive immune response to foreign antigens. This notion has shifted tremendously over the past decade with the recent generation of LC-deficient mouse models that has enabled scientists to study *in vivo* functions of LC. It is now clear that LC function to modulate immunological responses given that mice that lack LC have an exacerbated cutaneous hypersensitivity reaction. Furthermore, our lab recently demonstrated the unexpected LC contribution to chemically induced DNA damage and tumor development using the LC deficient mouse model. On the other hand, UV exposure causes the majority of human nonmelanoma cutaneous cancers by inducing DNA damage and tumor promotion within keratinocytes. No previous studies have been able to realize the functional role of LC in UV exposed skin, even though we now have evidence that implicates these cells in carcinogenesis.

The experiments within this thesis are the first to demonstrate the pro-tumor effects of LC at several steps during photocarcinogenesis. We used the transgenic mouse model that constitutively lacks epidermal LC to show that LC deficiency protects against DNA damage at 1 hour following UVB exposure. To elucidate the mechanism of DNA damage in the presence of LC, we went on to show that the amount of pathognomonic direct and indirect DNA damage lesions that occur in the surrounding keratinocytes in the presence or absence of LC is not significantly different. Finally, we showed that LC deficiency also protects against the formation and growth of p53 islands following long-term and repeated UVB exposure.

Our new understanding of LC contribution to photocarcinogenesis can be divided into acute and chronic temporal events. Following acute UVB exposure, LC remain in close proximity with keratinocytes. These findings that LC are relatively resistant to the DNA-damaging effects of UV is in sharp contrast to prior literature suggesting that LC are particularly susceptible to UV irradiation (78). Previous studies, however, used significantly higher and repeated doses of UVB light that are not comparable to physiologic solar radiation thus forcing LC to migrate out of the epidermis or undergo apoptosis. We, on the other hand, observe LC present within the epidermis at 1 hour following low-dose UVB exposure, indicating that they are able to elicit effects on the surrounding environment at least within the first 1 to 24 hours after irradiation. It is precisely at this time during which we also see a significantly greater induction of DNA damage in the presence of LC as measured by γH2Ax.

The serine 139 phosphorylated variant of H2Ax has been used as a paradigm of double-stranded DNA breaks caused by ionizing radiation (79). Immunofluorescence of γH2Ax in the classical presentation has been described as discrete nuclear foci (80). It is possible that the elevated quantity of γH2Ax positive keratinocytes in LC intact mice may represent increased double-stranded DNA breaks. Our homogenous nuclear staining pattern without foci, however, may also suggest an alternative mechanism. In fact, distinct distribution phenotypes of γH2Ax have been correlated with different DNA damage processes. Others have shown that UV-irradiated cells display varying levels of pan-nuclear γH2Ax pattern that is independent of double-stranded DNA breaks and may be associated with survival or pre-apoptotic signaling (32, 81). The same researchers further demonstrated that UV-induced γH2Ax is dependent on nucleotide excision repair

(NER) signaling (82). NER is the predominant mechanism by which direct UV-induced DNA damage is repaired, including both CPD and 6,4-photoproducts (83). We, therefore, sought to verify the correlation between our γH2Ax data with CPD formation following acute UVB exposure.

Although we observe a UVB dose-dependent increase in CPD immunofluorescence, the absence of LC does not result in a reduction in CPD fluorescence intensity. This suggests that if the presence of LC contributes to γH2Ax DNA damage and/or signaling, it is not by a direct increase in CPD formation. The antibody we used for this immunofluorescence assay, however, is CPD-specific and does not provide insight into the possible importance of 6,4-photoproducts. Although they are a minor fraction of direct DNA lesions created in the presence of UVB, 6,4-photoproducts have been shown to be more mutagenic and have a slower repair rate that parallels γH2Ax repair kinetics (82). It may, therefore, be useful to examine the correlation of LC presence or absence with 6,4-photoproducts as an indicator of direct DNA damage.

In addition to the above, more recent studies demonstrated that γH2Ax is phosphorylated and recruited not only during NER signaling, but in particular when the NER machinery is disrupted (84). Accordingly, others have shown that dysfunctional CPD repair leads to single-stranded DNA intermediates and double-stranded DNA breaks (85). Thus, CPD formation may be LC independent, but proper NER-driven CPD repair may be affected by the presence of LC. Although we only briefly examined CPD immunofluorescence at 24 hours post irradiation, once CPD repair has been initiated as indicated by a decrease in CPD fluorescence, a more thorough investigation of LC effects

of direct DNA repair may be warranted. Such additional studies could include the investigation of CPD repair kinetics in LC-intact and LC deficient skin. One recent study proposed that CPD repair is inhibited by nitric oxide (NO) production (86). Both LC (87) and keratinocytes (88) have been shown to produce NO upon activation by lipopolysaccharide (in the LC study) or by UVB irradiation (in the keratinocyte study). It is possible that LC inhibit CPD repair by direct NO production or by modulating the production of NO by keratinocytes and it will, therefore, be valuable to measure NO production in UVB-irradiated skin in the absence and presence of LC.

Nevertheless, our CPD data led us to further investigate LC contribution to indirect UV-induced DNA damage with corresponding experiments using fluorescence probes. We demonstrate a trend of increased oxidative stress within KC in the presence of UVB-irradiated LC, several technical difficulties, however, have to be overcome to fully understand the results. First, CellROX Green fluorescence intensity within live cells revealed significant positional variability, thus affected by drift and cellular movement during image acquisition. We overcame this by averaging multiple fields for each time point rather than following one field over time. Second, although CellROX Green is cell membrane permeate to allow for loading into cells, we also observed significant fluorescence intensity dilution following the initial loading that may be artificially decreasing the indication of oxidative stress within cells. We overcame this problem by allowing cells to remain in the presence of CellROX Green for the duration of the image acquisition to prevent wash out. Consequently, our gradual increase in the fluorescence intensity at baseline may correspond to either physiological oxidation upon exposure to air and light in the environment or due to continued uptake of the fluorescent probe by

the cells. Third, CellROX Green is a non-specific marker providing a generalized indication of the oxidative status within a cell, however, provides little information on the specific ROS involved. The information gained from these experiments, nevertheless, is useful for future methodological development as well as interpreting literature that uses CellROX Green and similar DCFDA-type probes.

The technical difficulties that we encountered in the use of CellROX Green, however, led us to pursue other avenues to study indirect UV-induced DNA damage at later steps, namely in the quantification of oxidizing nucleotide lesions such as 8-oxoguanine. Our 8-oxoguanine immunofluorescence data suggests that indirect DNA damage is LC-independent during acute UVB exposure. We observed 8-oxoguanine immunofluorescence within distinct nuclear foci, which is consistent with published work showing accumulation of OGG1, a DNA glycosylase responsible for 8-oxoguanine repair, within nuclear speckles following UVA irradiation (76). Although, in this study, the authors did not show 8-oxoguanine colocalization within the nuclear speckles, their OGG1 staining pattern is strikingly similar to ours and suggests that our assay is sensitive enough to detect oxidative lesions within keratinocytes. Nevertheless, the large number of 8-oxoguanine lesions present within unirradiated skin leads us to speculate that the chemical method by which we separate the epidermal layer from the dermis prior to tissue fixation may itself be introducing a vast amount of oxidative damage, thereby saturating our ability to detect a difference between LC intact and deficient skin. It may, therefore, be useful to apply the 8-oxoguanine immunofluorescence staining protocol to different methods of tissue preparation with decreased extraneous oxidative damage unrelated to UVB exposure.

It is also conceivable that the difference we observed in the number of γH2Ax positive cells in the presence or absence of LC may not be due to either direct (CPD) or indirect (8-oxoguanine) DNA damage within keratinocytes at all. Interestingly, many γH2Ax-positive nuclei were observed to be close to LC, suggesting that LC may somehow transfer their DNA-damaging effects locally. Keratinocytes constitute the majority of cells within the epidermis and thus are the predicted recipients of LC-facilitated DNA damage in the presence of UVB. In mice, however, the DETC constitute a third major subpopulation of cells that also come in direct contact with LC. DETC should, therefore, also be considered as the target of LC-induced DNA damage in the presence of UVB exposure. Although LC contribution to chemical carcinogenesis was shown to be DETC-independent (30), this may be different in UVB-induced carcinogenesis. The *Tcrb*$^{-/-}$ *Tcrd*$^{-/-}$ knockout mouse model lacks DETC can be crossbred with transgenic Lang-DTA mice to study the implication of both LC and DETC in UV-induced DNA damage. We will use these mice to compare γH2Ax-positive cells in LC^{+} $DETC^{+}$, LC^{-} $DETC^{+}$, LC^{+} $DETC^{-}$, and LC^{-} $DETC^{-}$ mice.

In combination with our data on DNA damage following acute UVB exposure, we also demonstrate that LC facilitate photocarcinogenesis upon chronic UVB exposure. It has long been known that UV light is a unique carcinogen that leads to both tumor initiation and promotion with repeated exposure. Our p53 immunofluorescence data suggests that LC presence in skin also contributes to both these processes following long-term UVB exposure. The clonal patches of keratinocytes containing p53 mutations are both more numerous and larger in the presence of LC. The increased p53 island quantity suggests more individual DNA lesions that eventually progressed to mutagenesis.

Whether this is in direct association with the greater number of γH2Ax positive keratinocytes that we observed in early events of UVB-exposed LC intact mice, however, remains unclear. Although, given that the significant difference in p53 island number occurs only at 9 weeks and not at 5 weeks following chronic UVB exposure suggests that it is unrelated to γH2Ax. More interestingly, the area of keratinocytes with mutant p53 is more than two times greater in the presence of LC, suggesting that LC play a substantial role in clonal expansion. There are numerous potential pathways by which LC may promote the clonal expansion of mutagenic keratinocytes, for example by influencing their proliferation and apoptosis. Recent work showed that LC can induce the proliferation of IL-22 producing $CD4^+$ T cells, thereby triggering keratinocyte proliferation and epidermal hyperplasia and inflammation (89). Furthermore, $CD4^+$ T cells are strongly induced to express IL-22 in the presence of FICZ, a tryptophan-derived photoproduct, suggesting that IL-22 production is favored during UV irradiation (90). Although only speculation at this point, soluble mediators, such as IL-22, pose plausible avenues by which LC may play a role in UV-induced tumor promotion.

Taken together, our work sheds light on the complex interactions of various cells in skin during UVB exposure that culminates in skin cancers. Although DNA damage and accumulation of mutations specifically in keratinocytes gives rise to nonmelanoma skin cancers, LC have also been shown to play a substantial role through our group's previously published work on polycyclic aromatic hydrocarbon chemical carcinogenesis and our current data on photocarcinogenesis. Our understanding of these interesting cells is rapidly expanding in the relatively short amount of time since their discovery by Paul Langerhans less than 150 years ago. A clearer understanding of LC interactions within

their innate cellular environment may serve to protect us from the inflammatory, immunosuppressive, ageing, and carcinogenic properties of solar radiation.

References

1. Langerhans P. Ueber die Nerven der menschlichen Haut. *Archiv f pathol Anat*. 1868;44(2-3):325–337.

2. Ferreira-Marques J. Systema sensitivum intra-epidermicum. *Archiv für Dermatologie und Syphilis*. 1951;193(3):191–250.

3. Tarnowski WM, Hashimoto K. Langerhans“ cell granules in histiocytosis X. The epidermal Langerhans” cell as a macrophage. *Arch Dermatol*. 1967;96(3):298–304.

4. Hashimoto K, Tarnowski WM. Some new aspects of the Langerhans cell. *Arch Dermatol*. 1968;97(4):450–464.

5. Zelickson AS. The Langerhans Cell. *J Invest Dermatol*. 44(3):201–212.

6. Silberberg-Sinakin I, Thorbecke GJ, Baer RL, Rosenthal SA, Berezowsky V. Antigen-bearing Langerhans cells in skin, dermal lymphatics and in lymph nodes. *Cell Immunol*. 1976;25(2):137–151.

7. Rowden G, Lewis MG, Sullivan AK. Ia antigen expression on human epidermal Langerhans cells. *Nature*. 1977;268:247–248.

8. Klareskog L, Tjernlund UM, Forsum U, Peterson PA. Epidermal Langerhans cells express Ia antigens. *Nature*. 1977;268:248–250.

9. Stingl G, Wolff-Schreiner EC, Pichler WJ, Gschnait F, Knapp W, Wolff K. Epidermal Langerhans cells bear Fc and C3 receptors. *Nature*. 1977;268(5617):245–246.

10. Banchereau J, Steinman RM. Dendritic cells and the control of immunity. *Nature*. 1998;392(6673):245–252.

11. Schuler G, Steinman RM. Murine epidermal Langerhans cells mature into potent immunostimulatory dendritic cells in vitro. *J Exp Med*. 1985;161(3):526–546.

12. Bauer J, Bahmer FA, Wörl J, Neuhuber W, Schuler G, FartaschM. A strikingly constant ratio exists between Langerhans cells and other epidermal cells in human skin. A stereologic study using the optical disector method and the confocal laser scanning microscope. *J Invest Dermatol*. 2001;116(2):313–318.

13. Nishibu A, Ward BR, Jester JV, Ploegh HL, Boes M, Takashima A. Behavioral Responses of Epidermal Langerhans Cells In Situ to Local Pathological Stimuli. *J Invest Dermatol*. 2006;126(4):787–796.

14. Kubo A, Nagao K, Yokouchi M, Sasaki H, Amagai M. External antigen uptake by Langerhans cells with reorganization of epidermal tight junction barriers. *J Exp Med*. 2009;206(13):2937–2946.

15. Girardi M, Lewis J, Glusac E, Filler RB, Geng L, Hayday AC, Tigelaar RE. Resident skin-specific gammadelta T cells provide local, nonredundant regulation of cutaneous inflammation. *J*

Exp Med. 2002;195(7):855–867.

16. Reis e Sousa C, Stahl PD, Austyn JM. Phagocytosis of antigens by Langerhans cells in vitro. *J Exp Med*. 1993;178(2):509–519.

17. Romani N, Koide S, Crowley M, Witmer-Pack M, Livingstone AM, Fathman CG, Inaba K, Steinman RM. Presentation of exogenous protein antigens by dendritic cells to T cell clones. *J Exp Med*. 1989;169(3):1169–1178.

18. Macatonia SE, Hosken NA, Litton M, Vieira P, Hsieh CS, Culpepper JA, Wysocka M, Trinchieri G, Murphy KM, O'Garra A. Dendritic cells produce IL-12 and direct the development of Th1 cells from naive CD4+ T cells. *J Immunol*. 1995;154(10):5071–5079.

19. Stoitzner P, Tripp CH, Eberhart A, Price KM, Jung JY, Bursch L, Ronchese F, Romani N. Langerhans cells cross-present antigen derived from skin. *Proc Natl Acad Sci USA*. 2006;103(20):7783–7788.

20. Flacher V, Sparber F, Tripp C, Romani N, Stoitzner P. Targeting of epidermal Langerhans cells with antigenic proteins: attempts to harness their properties for immunotherapy. *Cancer Immunol Immunother*. 2009;58(7):1137–1147.

21. Valladeau J, Ravel O, Dezutter-Dambuyant C, Moore K, Kleijmeer M, Liu Y, Duvert-Frances V, Vincent C, Schmitt D, Davoust J, Caux C, Lebecque S, Saeland S. Langerin, a novel C-type lectin specific to Langerhans cells, is an endocytic receptor that induces the formation of Birbeck granules. *Immunity*. 2000;12(1):71–81.

22. Douillard P, Stoitzner P, Tripp CH, Clair-Moninot V, Aït-Yahia S, McLellan AD, Eggert A, Romani N, Saeland S. Mouse Lymphoid Tissue Contains Distinct Subsets of Langerin/CD207+ Dendritic Cells, Only One of Which Represents Epidermal-Derived Langerhans Cells. *J Invest Dermatol*. 2005;125(5):983–994.

23. Kaplan DH, Jenison MC, Saeland S, Shlomchik WD, Shlomchik MJ. Epidermal Langerhans Cell-Deficient Mice Develop Enhanced Contact Hypersensitivity. *Immunity*. 2005;23(6):611–620.

24. Steinman RM, Nussenzweig MC. Avoiding horror autotoxicus: the importance of dendritic cells in peripheral T cell tolerance. *Proc Natl Acad Sci USA*. 2002;99(1):351–358.

25. Filler RB, Roberts SJ, Girardi M. Cutaneous Two-Stage Chemical Carcinogenesis. *CSH Protoc*. 2007;2007(9):pdb.prot4837.

26. Abel EL, Angel JM, Kiguchi K, DiGiovanni J. Multi-stage chemical carcinogenesis in mouse skin: Fundamentals and applications. *Nat Protoc*. 2009;4(9):1350–1362.

27. Ravindra K, Sokhi R, Van Grieken R. Atmospheric polycyclic aromatic hydrocarbons: Source attribution, emission factors and regulation. *Atmospheric Environment*. 2008;42(13):2895–2921.

28. Hennings H, Glick AB, Lowry DT, Krsmanovic SL, Sly LM, Yuspa SH. FVB/N mice: an inbred strain sensitive to the chemical induction of squamous cell carcinomas in the skin. *Carcinogenesis*. 1993;14(11):2353–2358.

29. DiGiovanni J. Multistage carcinogenesis in mouse skin. *Pharmacol Ther*. 1992;54(1):63–128.

30. Modi BG, Neustadter J, Binda E, Lewis J, Filler RB, Roberts SJ, Kwong BY, Reddy S, Overton JD, Galan A, Tigelaar R, Cai L, Fu P, Shlomchik M, Kaplan DH, Hayday A, Girardi M. Langerhans cells facilitate epithelial DNA damage and squamous cell carcinoma. *Science*. 2012;335(6064):104–108.

31. Quintanilla M, Brown K, Ramsden M, Balmain A. Carcinogen-specific mutation and amplification of Ha-ras during mouse skin carcinogenesis. *Nature*. 1986;322(6074):78–80.

32. Cleaver JE. γH2Ax: biomarker of damage or functional participant in DNA repair "all that glitters is not gold!". *Photochem Photobiol*. 2011;87(6):1230–1239.

33. Ghissassi El F, Baan R, Straif K, Grosse Y, Secretan B, et al. A review of human carcinogens--part D: radiation. *Lancet Oncol*. 2009;10(8):751–752.

34. Wu S, Han J, Li W-Q, Li T, Qureshi AA. Basal-cell carcinoma incidence and associated risk factors in U.S. women and men. *Am J Epidemiol*. 2013;178(6):890–897.

35. Aszterbaum M, Epstein J, Oro A, Douglas V, LeBoit PE, Scott MP, Epstein EH. Ultraviolet and ionizing radiation enhance the growth of BCCs and trichoblastomas in patched heterozygous knockout mice. *Nature Medicine*. 1999;5(11):1285–1291.

36. Findlay GM. Ultra-violet light and skin cancer. *Lancet*. 1928;212(5491):1070–1073.

37. Newton R, Reeves G, Beral V, Ferlay J, Parkin D. Effect of ambient solar ultraviolet radiation on incidence of squamous-cell carcinoma of the eye. *The Lancet*. 1996;347(9013):1450–1451.

38. Osterlind A, Tucker MA, Stone BJ, Jensen OM. The Danish case-control study of cutaneous malignant melanoma. II. Importance of UV-light exposure. *Int J Cancer*. 1988;42(3):319–324.

39. Epstein FH, Gilchrest BA, Eller MS, Geller AC, Yaar M. The Pathogenesis of Melanoma Induced by Ultraviolet Radiation. *N Engl J Med*. 1999;340(17):1341–1348.

40. Popp S, Waltering S, Herbst C, Moll I, Boukamp P. UV-B-type mutations and chromosomal imbalances indicate common pathways for the development of Merkel and skin squamous cell carcinomas. *Int J Cancer*. 2002;99(3):352–360.

41. Unna, PG. Die Histopathologie der Hautkrankheiten. *Berlin, A. Hirschwald*, 1894:816.

42. Urbach F, Forbes PD, Davies RE, Berger D. Cutaneous photobiology: past, present and future. *J Invest Dermatol*. 1976;67(1):209–224.

43. Ganti AK, Kessinger A. Systemic therapy for disseminated basal cell carcinoma: an uncommon manifestation of a common cancer. *Cancer Treat Rev*. 2011;37(6):440–443.

44. Rogers HW, Weinstock MA, Harris AR, Hinckley MR, Feldman SR, Fleischer AB, Coldiron BM. Incidence estimate of nonmelanoma skin cancer in the United States, 2006. *Arch Dermatol*. 2010;146(3):283–287.

45. Housman TS, Feldman SR, Williford PM, Fleischer AB, Goldman ND, Acostamadiedo JM,

Chen GJ. Skin cancer is among the most costly of all cancers to treat for the Medicare population. *J Am Acad Dermatol*. 2003;48(3):425–429.

46. Christenson LJ, Borrowman TA, Vachon CM, Tollefson MM, Otley CC, Weaver AL, Roenigk RK. Incidence of basal cell and squamous cell carcinomas in a population younger than 40 years. *JAMA*. 2005;294(6):681–690.

47. Karagas MR, Greenberg ER, Spencer SK, Stukel TA, Mott LA. Increase in incidence rates of basal cell and squamous cell skin cancer in New Hampshire, USA. New Hampshire Skin Cancer Study Group. *Int J Cancer*. 1999;81(4):555–559.

48. Brewster DH, Bhatti LA, Inglis JHC, Nairn ER, Doherty VR. Recent trends in incidence of nonmelanoma skin cancers in the East of Scotland, 1992–2003. *Br J Dermatol*. 2007;156(6):1295–1300.

49. Staples MP, Elwood M, Burton RC, Williams JL, Marks R, Giles G. Non-melanoma skin cancer in Australia: the 2002 national survey and trends since 1985. *Med J Aust*. 2006;184(1):6–10.

50. Euvrard S, Kanitakis J, Claudy A. Skin cancers after organ transplantation. *N Engl J Med*. 2003;348(17):1681–1691.

51. Sutherland JC, Griffin KP. Absorption spectrum of DNA for wavelengths greater than 300 nm. *Radiation research*. 1981;86(3):399–410.

52. Freeman RG, Hudson HT, Carnes R. Ultraviolet wavelength factors in solar radiation and skin cancer. *Int J Dermatol*. 1970;9(3):232–235.

53. Freeman RG. Data on the Action Spectrum for Ultraviolet Carcinogenesis. *J Natl Cancer Inst*. 1975;55(5):1119–1122.

54. Kappes UP, Luo D, Potter M, Schulmeister K, Rünger TM. Short- and Long-Wave UV Light (UVB and UVA) Induce Similar Mutations in Human Skin Cells. *J Invest Dermatol*. 2006;126(3):667–675.

55. Rünger TM. Role of UVA in the pathogenesis of melanoma and non-melanoma skin cancer: A short review. *Photodermatol Photoimmunol Photomed*. 1999;15(6):212–216.

56. Ikehata H, Higashi S, Nakamura S, Daigaku S, Furusawa Y, Kamei Y, Watanabe M, Yamamoto K, Hieda K, Munakata N. Action spectrum analysis of UVR genotoxicity for skin: the border wavelengths between UVA and UVB can bring serious mutation loads to skin. *J Invest Dermatol*. 2013;133(7):1850–1856.

57. Cadet J, Sage E, Douki T. Ultraviolet radiation-mediated damage to cellular DNA. *Mutat Res*. 2005;571(1-2):3–17.

58. Mitchell DL. The relative cytotoxicity of (6-4) photoproducts and cyclbutane dimers in mammalian cells. *Photochem Photobiol*. 1988;48(1):51–57.

59. Franklin WA, Haseltine WA. The role of the (6−4) photoproduct in ultraviolet light-induced transition mutations in E. coli. *Mutation Research/DNA Repair Reports*. 1986;165(1):1–7.

60. Yarosh D, Alas LG, Yee V, Oberyszyn A, Kibitel JT, Mitchell D, Rosenstein R, Spinowitz A, Citron M. Pyrimidine dimer removal enhanced by DNA repair liposomes reduces the incidence of UV skin cancer in mice. *Cancer Res*. 1992;52(15):4227–4231.

61. Yagi T, Morimoto T, Takebe H. Correlation of (6-4)photoproduct formation with transforming mutations in UV-irradiated Ha-ras. *Carcinogenesis*. 1995;16(4):689–695.

62. Danpure HJ, Tyrrell RM. Oxygen-dependence of near UV (365 nm) lethality and the interaction of near UV and X-rays in two mammalian cell lines. *Photochem Photobiol*. 1976;23(3):171–177.

63. Nishimura H, Yasui H, Sakurai H. Generation and distribution of reactive oxygen species in the skin of hairless mice under UVA: studies on in vivo chemiluminescent detection and tape stripping methods. *Experimental Dermatol*. 2006;15(11):891–899.

64. Masaki H, Izutsu Y, Yahagi S, Okano Y. Reactive oxygen species in HaCaT keratinocytes after UVB irradiation are triggered by intracellular Ca(2+) levels. *J Investig Dermatol Symp Proc*. 2009;14(1):50–52.

65. Cadet J, Douki T, Gasparutto D, Ravanat J-L. Oxidative damage to DNA: formation, measurement and biochemical features. *Mutat Res*. 2003;531(1–2):5–23.

66. Le Page F, Margot A, Grollman AP, Sarasin A, Gentil A. Mutagenicity of a unique 8-oxoguanine in a human Ha-ras sequence in mammalian cells. *Carcinogenesis*. 1995;16(11):2779–2784.

67. Bjelland S, Seeberg E. Mutagenicity, toxicity and repair of DNA base damage induced by oxidation. *Mutat Res*. 2003;531(1-2):37–80.

68. Vousden KH, Lane DP. p53 in health and disease. *Nat Rev Mol Cell Biol*. 2007;8(4):275–283.

69. Donehower LA, Harvey M, Slagle BL, McArthur MJ. Mice deficient for p53 are developmentally normal but susceptible to spontaneous tumours. *Nature*. 1992;

70. Ziegler A, Jonason AS, Leffell DJ, Simon JA, Sharma HW, Kimmelman J, Remington L, Jacks T, Brash DE. Sunburn and p53 in the onset of skin cancer. *Nature*. 1994;372(6508):773–776.

71. Brash DE, Rudolph JA, Simon JA, Lin A, McKenna GJ, Baden HP, Halperin AJ, Pontén J. A role for sunlight in skin cancer: UV-induced p53 mutations in squamous cell carcinoma. *Proc Natl Acad Sci USA*. 1991;88(22):10124–10128.

72. Olive KP, Tuveson DA, Ruhe ZC, Yin B, Willis NA, Bronson RT, Crowley D, Jacks T. Mutant p53 gain of function in two mouse models of Li-Fraumeni syndrome. *Cell*. 2004;119(6):847–860.

73. Benavides F, Oberyszyn TM, VanBuskirk AM, Reeve VE, Kusewitt DF. The hairless mouse in skin research. *J Dermatol Sci*. 2009;53(1):10–18.

74. Diffey BL, Jansen CT, Urbach F, Wulf HC. The standard erythema dose: a new photobiological concept. *Photodermatol Photoimmunol Photomed*. 1997;13(1-2):64–66.

75. Seité S, Zucchi H, Doyal M, Tison S, Compan D, Christiaens F, Gueniche A, Fourtanier A. Alterations in human epidermal Langerhans cells by ultraviolet radiation: quantitative and morphological study. *Br J Dermatol*. 2003;148(2):291–299.

76. Campalans A, Amouroux R, Bravard A, Epe B, Radicella JP. UVA irradiation induces relocalisation of the DNA repair protein hOGG1 to nuclear speckles. *Journal of Cell Science*. 2007;120(1):23–32.

77. Merad M, Manz MG, Karsunky H, Wagers A, Peters W, Charo I, Weissman IL, Cyster JG, Engleman EG. Langerhans cells renew in the skin throughout life under steady-state conditions. *Nat Immunol*. 2002;3(12):1135–1141.

78. Aberer W, Schuler G, Stingl G, Hönigsmann H, Wolff K. Ultraviolet light depletes surface markers of Langerhans cells. *J Invest Dermatol*. 1981;76(3):202–210.

79. Rogakou EP, Pilch DR, Orr AH, Ivanova VS, Bonner WM. DNA double-stranded breaks induce histone H2AX phosphorylation on serine 139. *J Biol Chem*. 1998;273(10):5858–5868.

80. Paull TT, Rogakou EP, Yamazaki V, Kirchgessner CU, Gellert M, Bonner WM. A critical role for histone H2AX in recruitment of repair factors to nuclear foci after DNA damage. *Curr Biol*. 2000;10(15):886–895.

81. de Feraudy S, Revet I, Bezrookove V, Feeney L, Cleaver JE. A minority of foci or pan-nuclear apoptotic staining of H2AX in the S phase after UV damage contain DNA double-strand breaks. *Proc Natl Acad Sci USA*. 2010;107(15):6870–6875.

82. Marti TM, Hefner E, Feeney L, Natale V, Cleaver JE. H2AX phosphorylation within the G1 phase after UV irradiation depends on nucleotide excision repair and not DNA double-strand breaks. *Proc Natl Acad Sci USA*. 2006;103(26):9891–9896.

83. Hoeijmakers JH. Genome maintenance mechanisms for preventing cancer. *Nature*. 2001;411(6835):366–374.

84. Matsumoto M, Yaginuma K, Igarashi A, Imura M, Hasegawa M, Iwabuchi K, Date T, Mori T, Ishizaki K, Yamashita K, Inobe M, Matsunaga T. Perturbed gap-filling synthesis in nucleotide excision repair causes histone H2AX phosphorylation in human quiescent cells. *J Cell Sci*. 2007;120(6):1104–1112.

85. Garinis GA, Mitchell JR, Moorhouse MJ, Hanada K, de Waard H. Transcriptome analysis reveals cyclobutane pyrimidine dimers as a major source of UV-induced DNA breaks. *EMBO J*. 2005;24(22):3952–3962.

86. Ding W, Hudson LG, Sun X, Feng C, Liu KJ. As(III) inhibits ultraviolet radiation-induced cyclobutane pyrimidine dimer repair via generation of nitric oxide in human keratinocytes. *Free Radic Biol Med*. 2008;45(8):1065–1072.

87. Qureshi AA, Hosoi J, Xu S, Takashima A, Granstein RD, Lerne EA. Langerhans Cells Express Inducible Nitric Oxide Synthase and Produce Nitric Oxide. *J Invest Dermatol*. 1996;107(6):815–821.

88. Deliconstantinos G, Villiotou V, Stravrides JC. Release by ultraviolet B (u.v.B) radiation of

nitric oxide (NO) from human keratinocytes: a potential role for nitric oxide in erythema production. *Bri J Pharmacol*. 1995;114(6):1257–1265.

89. Fujita H, Nograles KE, Kikuchi T, Gonzalez J, Carucci J, Krueger JG. Human Langerhans cells induce distinct IL-22-producing CD4+ T cells lacking IL-17 production. *Proc Natl Acad Sci USA*. 2009;106(51):21795–21800.

90. Veldhoen M, Duarte JH. The aryl hydrocarbon receptor: fine-tuning the immune-response. *Curr Opin Immunol*. 2010;22(6):747–752.